Electric-field-induced electron detachment of 800-MeV H^- ions

P. B. Keating, M. S. Gulley, H. C. Bryant, E. P. MacKerrow, W. A. Miller, and D. C. Rislove
University of New Mexico, Albuquerque, New Mexico 87131

Stanley Cohen, J. B. Donahue, D. H. Fitzgerald, David J. Funk, S. C. Frankle, R. L. Hutson, R. J. Macek, M. A. Plum, N. G. Stanciu, O. B. van Dyck, and C. A. Wilkinson
Los Alamos National Laboratory, Los Alamos, New Mexico 87545

(Received 16 June 1995)

The lifetime of 800-MeV H^- ions against electron detachment in a static electric field was measured over a range of eight orders of magnitude in experiments at the High Resolution Atomic Beam Facility of the Los Alamos Meson Physics Facility. The ions traversed a linear gradient magnetic field of 1.3-T peak strength resulting in a 6-MV/cm peak rest-frame electric field capable of stripping a large fraction of H^- ions. The unstripped H^- ions, neutral H^0 atoms, and protons were detected 5.5 m from the magnet. This spectrum was analyzed to determine the lifetime of the H^- ion versus electric-field strength and the results were compared with previous studies. Three parametrizations of the lifetime formula based on an existing theory were used to calculate the stripping probability. The data were fit to the lifetime formula and good agreement with theoretical predictions was found. Finally, a possible experiment for observing excited states of H^- is briefly discussed.

PACS number(s): 34.90.+q, 41.75.Cn, 32.70.Cs, 32.80.Gc

I. INTRODUCTION

The lifetime of the only experimentally observed bound state of the H^- ion ($1s^2\ ^1S$) against electron detachment in an electric field has been investigated by theoreticians and experimentalists for years [1–3]. The electron affinity of this state is 0.75419(2) eV [4,5]. The low binding energy imposes constraints on the strength of bending magnets and beam energies of accelerators using this ion. If the motional electric field produced by a bending magnet is too strong, the ion may strip to neutral H^0 causing problems for the accelerator. In this work, the transformation of a magnetic field to a strong rest-frame electric field is used to our advantage. The motional electric field produced with our laboratory magnetic field is capable of ionizing the H^- ion, and is used to measure the H^- lifetime in the field. The magnetic field used in this work increased linearly with distance along the beam direction (taken to be the z direction) and produced rest-frame electric-field strengths from 0 to 6 MV/cm. The H^- ion lifetime as a function of field was determined by measuring the population of H^- ions stripped in the field as a function of distance transverse to the incident beam direction (taken to be the x direction).

Previous work by Stinson *et al.* (Ref. [1]) performed at the Rutherford High Energy Laboratory was at the much lower beam energy of 49.5 MeV and used a magnet with a peak field of 2.18 T. A position-sensitive acoustic spark chamber was used for H^- ion detection. The work of Jason *et al.* (Ref. [3]) performed at the Los Alamos Meson Physics Facility (LAMPF) used much of the same equipment and similar beam characteristics as were used in our experiment. The main difference in experimental apparatus between our study and the Jason *et al.* study was that Jason *et al.* used a multiwire proportional chamber (MWPC), and we used scintillator detectors.

This study of single electron detachment of H^- in strong motional electric fields was a byproduct of a study to measure production of excited H^0 states and single and double electron detachment of H^- using C and Al_2O_3 foils [6]. Although the main motivation for this set of experiments was with the interaction of 800-MeV H^- ions with thin foils, studying the H^- stripping and comparing with previous experimental results of Jason *et al.* was useful as a check of our experimental apparatus.

The second bound state of the H^- ion, the $2p^2\ ^3P^e$ state, proposed by Holøien [7] and studied by Drake [8], has never been experimentally verified. Using a variational calculation, Drake calculated a lower bound on the energy of this state to be approximately 9.5 meV. The state may be formed by radiative attachment or by collisional excitation with spin flip from the ground state ^1S. The $2p^2\ ^3P^e$ state could radiate into the $1skp\ ^3P$ continuum or to the $2s2p\ ^3P$ autoionizing state with a lifetime of about 1.73 ns.

The possibility of observing a long-lived ($\sim$1 ns) state of H^- produced in a foil was another motivation for the experiment. In the measurement used for determining H^- field detachment, the H^- beam was incident on a thin C foil (surface density 9 μg/cm^2). While the foil was not necessary for measuring H^- field detachment, it was well suited for the study since the relatively thin foil stripped only a small fraction of incident H^- ions leaving a large fraction of unstripped ions to be stripped in the motional electric field produced by the magnet. Furthermore, we were interested in the possibility of observing H^- excited states produced when an H^- ion beam interacts with a thin foil. We will examine whether the $2p^2\ ^3P^e$ state of H^- could have been observed in our data.

In all that follows, the direct effects of magnetic fields on the ions have been neglected; only the motional electric fields are used in the calculations of the lifetime against field detachment.

II. THEORY

The lifetime of an H^- ion in a weak static electric field F was calculated by Scherk (Ref. [2]) to be

$$\tau=\frac{4mz_T}{S_0N^2\hbar(1+p)^2\left(1-\frac{1}{2k_0z_T}\right)}\exp\left(\frac{4k_0z_T}{3}\right), \quad (1)$$

where the spectroscopic coefficient $S_0=0.794$. The normalization constant N is given by

$$N=\frac{[2k_0(k_0+\alpha)(2k_0+\alpha)]^{1/2}}{\alpha}, \quad (2)$$

where α is a parameter based on the work by Tietz [9], who developed an ionic potential function used in calculating N. The ionic potential, representing the average interaction of the ionic electron with the daughter atom, has the form $V_1(\mathbf{r})=-V_0[e^{-\alpha r}/(1-e^{-\alpha r})]$, where r is the distance from the ionic electron to the core. The potential function was required to give the correct electron affinity and to approximate the Hartree field at large distance, resulting in values of $V_0=68.2$ eV and $\alpha=3.81\times10^8$ cm^{-1}. The factor p accounts for the polarization of the ionic wave function and has the value 0.0126 based on perturbation theory. The parameter k_0 appears in the ionic wave function (an s wave) whose asymptotic form is proportional to $[\exp(-k_0r)]/r$. The factor k_0 is determined from the relation $k_0^2=2m(-\varepsilon_0)/\hbar^2$. The classical outer turning radius $z_T=-\varepsilon_0/eF$. For a field of 2MV/cm, z_T is approximately 38 Å. The electron affinity ε_a is related to ε_0 and the level shift $D(\varepsilon_0)$ by $\varepsilon_a=-\varepsilon_0+D(\varepsilon_0)$. Scherk estimated the value of $D(\varepsilon_0)$ to be $-0.000\,41$ eV. The value of S_0 was obtained by Scherk using a 49-parameter wave function. Scherk estimated the lifetime value to be accurate to about 1% for a field strength of 2 MV/cm.

III. EXPERIMENTAL METHOD

The basic experimental setup is shown in Fig. 1. The typical momentum spread of the LAMPF H^- beam was estimated to be $\delta p/p\sim5\times10^{-4}$ based on previous experiments. The beam energy was not measured directly for these experiments, but a nominal value of 797 ± 2 MeV was typical for the High Resolution Atomic Beam Facility (HIRAB) laboratory at LAMPF. The macropulse rate was 118 Hz, and the macropulse length was 725 μs, with a hybrid structure consisting of a repeated pattern of 35 ns of 5-ns spaced micropulses, followed by 65 ns without micropulses.

The strong rest-frame electric field used to strip the H^- ions was produced with a laboratory electromagnet. According to the Lorentz transformation, a laboratory magnetic field $\mathbf{B}_{\rm lab}$ produces a rest-frame electric field,

$$\mathbf{F}_{\rm rest}=\gamma\mathbf{v}\times\mathbf{B}_{\rm lab}, \quad (3)$$

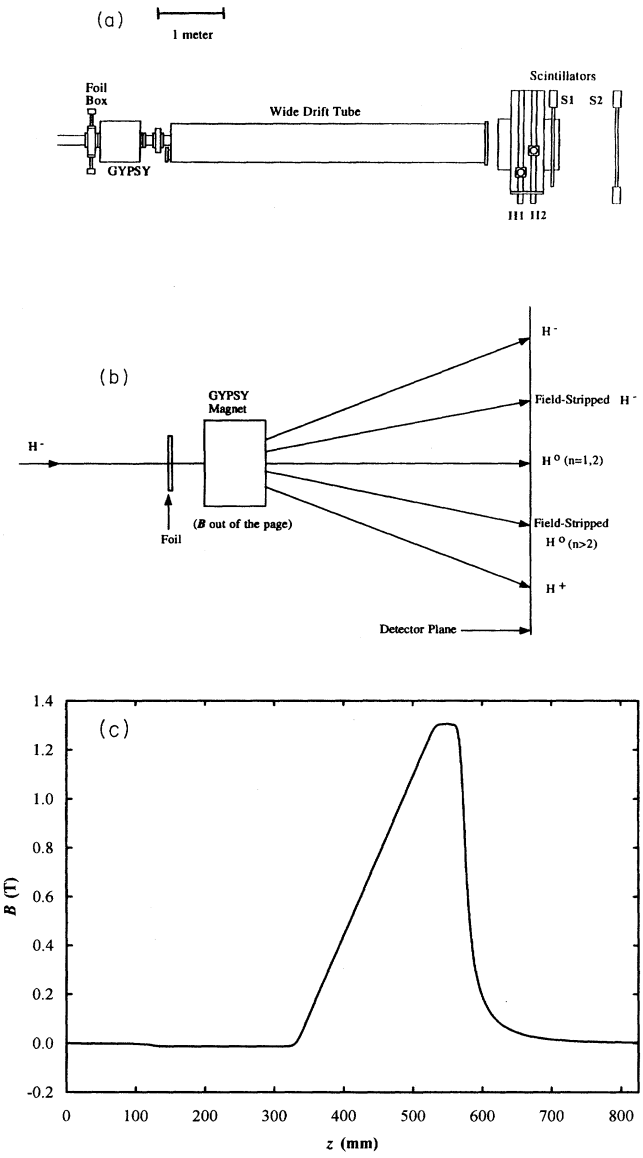

FIG. 1. (a) Schematic diagram (roughly to scale) of experimental apparatus showing the beam line, the stripping magnet, and locations of the detectors. The H^- beam of nominal energy 797 MeV impinges on the foil upstream of the linear gradient magnet "Gypsy" where the H^- are stripped. Scintillators $S1$ and $S2$ form a fixed telescope in coincidence with the scanning scintillator $H2$. A second scanning scintillator $H1$ shown in the figure was not used in this work. (b) Diagram showing the possible outcomes of interactions of H^- incident on the foil followed by traversal through the field of the "Gypsy" magnet. The various charge states are separated and detected 5.5 m from the peak magnetic field with the scanning scintillator $H2$ in coincidence with two wide fixed scintillators $S1$ and $S2$ covering the whole spectrum. The scanning scintillator travels in fixed increments along the x direction, the magnetic-field points in the negative y direction, and the incident beam defines the z direction. (c) The magnetic field of the "Gypsy" magnet (negative y direction) as a function of distance along the beam direction (z direction), for a fixed voltage drop across the shunt through which that current that excited the magnet passed.

where $\mathbf{v}$ is the ion's velocity in the laboratory frame, $\gamma = T/Mc^2 + 1$, T is the kinetic energy of the beam, and Mc^2 is the rest energy of the H^- ion. For a beam energy of 797 MeV ($\gamma = 1.85$), a 1 T laboratory magnetic field results in a rest-frame electric field of 4.67 MV/cm.

The magnet used for the experiments is called the "Gypsy" and is the same magnet used by Jason *et al.* (Ref. [3]). The Gypsy is a half-quadrupole magnet turned 90° from the usual orientation of a quadrupole producing a field that increased linearly with distance, as shown in Fig. 1(c). The field was set remotely to approximately 13 kG and the peak field was monitored with a shunt resistor whose output voltage was used in the calibration of the magnet. The field direction (y direction) was downward, perpendicular to the laboratory floor.

A 5-m-long stainless steel, rectangular cross-section drift tube was located downstream of the magnet. The 5-mil-thick aluminum exit window stripped all particles of electrons.

Scintillators downstream of the exit window were used to detect the protons derived from unstripped H^- ions and neutral H^0 atoms as shown in Fig. 1(a). Scintillators were chosen instead of a wire chamber for their simplicity, linear response for high counting rates, and faster readout time when coupled with standard CAMAC electronics. Two wide scintillators (called $S1$ and $S2$) in fixed positions and in temporal coincidence with a 5.84-mm-wide "scanning" scintillator, called $H2$, were used to obtain the spectrum shown in Fig. 3. The scintillators $S1$ and $S2$ counted all particles emerging from the exit window and were used for normalization. The normalized spectrum shown in Fig. 3(a) is the coincidence between $H2$, $S1$, and $S2$, divided by the coincidence between $S1$ and $S2$, denoted by $(H2 \cdot S1 \cdot S2)/(S1 \cdot S2)$. A second scanning scintillator, called $H1$, used in the foil studies (Ref. [6]) was not used in this experiment. The coincidence between scintillators $H2$, $S1$, and $S2$ discriminated against unwanted background signals. The scanning scintillator was mounted on a translation stage coupled to a drive screw. The drive screw was turned by a stepper motor controlled by a personal computer. The two wide scintillators $S1$ and $S2$ covered the entire exit window and counted all unstripped H^-, H^0, and H^+ particles. A data point was taken at a fixed $H2$ location until the $S1$ signal reached a set maximum number of counts (about 650 000). With the beam parameters listed above, the probability of double counting was below 10^{-4}. After completing an individual point, the personal computer-actuated stepping motor moved the scanning scintillator 3 mm along the x direction and another data point was recorded until the region from the H^- peak to the proton peak was covered as shown in Fig. 3(a).

The personal computer also controlled the data acquisition via interface with standard fast electronic components (CAMAC modules). The HIRAB laboratory beam line pressure was approximately 10^{-7} torr.

IV. DATA ANALYSIS

A. Calculations based on dP/dx vs x for stripped H^-

There were two main parts of the analysis procedure. The first was to calculate the stripping probability as a function of field, and the second was to determine the distribution of stripped H^- as a function of distance along the travel direction of the scanning scintillator.

The parametrized lifetime formula of Scherk (Ref. [2]) was used to calculate the H^- stripping probability as a function of field. The probability density distribution function was calculated for a grid of parameter values, as described below, and the calculations were then compared with the experimental results. This technique is different from the analysis of Stinson *et al.*, who calculated the lifetime in two ways, called the "strip" and "integral" methods. The "strip" method used only the center region of the observed spectra, and the "integral" method depended on the total number of stripped ions in the spectra. The technique of fitting the probability density distribution function directly (that is, without integrating the probability density distribution function) is useful since it is possible to determine systematic differences between the data and the Scherk theory as a function of field.

The magnet map was divided along the z direction (incident beam direction) into cells of uniform size. The decrease in population ΔP of H^- due to electron detachment through the ith cell is given by

$$\Delta P_i = P_0 \exp\left(-\frac{\Delta t_i}{\tau_i}\right), \tag{4}$$

where P_0 is the population entering the cell, Δt_i is the rest-frame transit time through cell i, and τ_i is the rest-frame lifetime in cell i. τ_i depends on the electric field $F(z_i)$ and other variables in the lifetime formula, depending on parametrization. The H^0 atoms derived from H^- ions that decayed in cell i were detected uniquely at scanning scintillator location x_i.

The number of H^- ions expected to decay would depend on the lifetime formula [Eq. (1)], which was parametrized in three different ways. The simplest parametrization (denoted $P1$), an approximation to the lifetime formula, was

$$\tau = \frac{a}{F} \exp\left(\frac{b}{F}\right), \tag{5}$$

where a and b were constants whose values were to be determined. Jason *et al.* also used the parametrization $P1$ of Eq. (5).

The second parametrization used (denoted $P2$), also an approximation to the lifetime formula, was

$$\tau = \frac{a_F}{(1-\eta F)F} \exp\left(\frac{b_F}{F}\right), \tag{6}$$

where η has the value 1.4901×10^{-10} m/V when the theoretical values of S_0, ε_0, p, and α, cited by Scherk, are used. This parametrization was used to determine the effects of the field dependence on the factor multiplying the exponential. For 797 MeV, the factor η equals 7×10^{-2}/T in the lab frame, and is non-negligible in the case of strong fields.

Finally, the lifetime formula [Eq. (1)] was written in terms of $\varepsilon = -\varepsilon_0$, α, and S_0 as

$$\tau(\varepsilon,S_0,\alpha)=\frac{4m\left(\frac{\varepsilon}{e}\right)^{1/2}}{S_0\hbar[N(\alpha,\varepsilon)]^2(1+p)^2\left(1-\frac{F}{\varepsilon^{3/2}\left(\frac{8m}{e^2\hbar^2}\right)^{1/2}}\right)}\frac{1}{F}\exp\left[\frac{2}{3}\left(\frac{8m}{e^2\hbar^2}\right)^{1/2}\frac{\varepsilon^{3/2}}{F}\right]. \tag{7}$$

Writing N in terms of α and ε, Eq. (7) becomes

$$\tau(\varepsilon,S_0,\alpha)=\frac{\sqrt{2\varepsilon}m\alpha^2}{S_0(1+p)^2e\left(\frac{\sqrt{2\varepsilon}}{\hbar}+\alpha\right)\left(\frac{\sqrt{8\varepsilon}}{\hbar}+\alpha\right)\left(1-\frac{\sqrt{2}\hbar eF}{4\sqrt{m}\varepsilon^{3/2}}\right)}\frac{1}{F}\exp\left[\frac{2}{3}\left(\frac{8m}{e^2\hbar^2}\right)^{1/2}\frac{\varepsilon^{3/2}}{F}\right]. \tag{8}$$

This parametrization, denoted $P3$, made no approximations to the lifetime formula of Eq. (1).

The second part of the analysis procedure concerned the trajectories of the various charge species through the magnet and to the detector plane. The calculations were done in the laboratory frame where the equations of motion were simple. The trajectory calculation was based on the Gypsy magnet field map measured in $\frac{1}{4}$-in. (6.35-mm) intervals for 825.5 mm. A cubic spline fit to the field map composed of 1651 points (for 0.5-mm intervals along the z direction) was used initially as input to a spreadsheet program that calculated the probability density distribution functions for the stripped H^- based on the lifetime formula. The trajectory algorithm was checked for the case of a constant and static field, where the analytic solution was compared with the discrete step algorithm. The analytic calculation and the discrete-step algorithm agreed. An algorithm was also written for the case of a uniformly ramped field and the stepwise method agreed with the analytical result. The constant field algorithm, with an average field computed for each cell, was compared with the ramped field algorithm for the case of a ramped field and the two agreed within a few parts in 10^7. After these initial tests, the step size in the linear region of the field map from 0.4 to 1.25 T was reduced to 0.05 mm resulting in a lower χ^2 as compared with the coarser step size. The results reported use the 0.05-mm step size in the linear region of the magnet map.

The trajectory calculation described above was based on a single-ion code. In order to compare the theoretical predictions with the experimental data, the finite beam width [$\sim$1 mm full width at half maximum (FWHM)] and the detector response function were convolved with the theoretical predictions. The detector response function and the ion beam width were determined from a multiparameter fit using a modified Levenberg-Marquardt algorithm [10] on data obtained in runs taken with a small step size designed to determine the beam profile. The detector was modeled as having a straight-edged response with a Gaussian top, and both the width of the straight-edged part and the Gaussian width were varied. The ion beam was assumed to be Gaussian. The two other variable parameters were an arbitrary normalization factor and a shift parameter which specified the peak of the convolution. The beam width and the detector response function parameters from the fitting procedure were used later for convolving with the theoretical probability distribution functions. The detector width determined from the fit was close to the measured width of the plastic scintillator material of the scanning scintillator, and the beam width was also close to the width measured in previous experiments.

The peak separation depended on the field setting and the beam energy. The voltage drop across a calibrated shunt was used to indicate the peak field of the magnet. When the calculations for different beam energies were made, the distance from the Gypsy magnet to the detector was adjusted ($\sim$6 cm in the z direction) to match the observed H^0 to H^+ peak separation.

The x positions of the theoretical predictions for each pair of fitting coefficients and a fixed magnetic-field setting were matched with the experimental data and a χ^2 was calculated with the goal of finding the coefficients that would minimize the χ^2. The standard deviations of the data points were relatively low due to the high number of particle counts obtained for each experimental data point. A χ^2 surface for beam energies of 795, 797, and 799 MeV was calculated using 36 experimental data points.

B. Analysis of the Stinson *et al.* results

We used the lifetime values of Stinson *et al.* to determine the parameters a and b of $P1$, a_F and b_F of $P2$, and S_0 and ε of $P3$. Stinson *et al.* obtained lifetime values as a function of field in two different ways, called the "strip" and "integral" methods. The fitting results for both methods are shown. Seven experimental data points were obtained (with one of the field values repeated) in the Stinson *et al.* study. The rest-frame electric fields ranged from 1.867 to 2.140 MV/cm with corresponding lifetimes of 416–19 μs. Calculations of χ^2 surfaces were made for $P1$ and $P2$ and the results, presented in Table III, will be discussed below. The relative insensitivity of the lifetime to the parameter α in $P3$ allowed a χ^2 surface to be calculated for the remaining parameters S_0 and ε.

V. RESULTS AND DISCUSSION

A. Results based on fitting the dP/dx distribution

The results of calculations for fitting the dP/dx distributions for parametrizations $P1$ and $P2$ to data of the present experiment are presented in Tables I and II and in Fig. 2. The reduced χ^2 for $P1$ was 1.18, which was higher than that for

TABLE I. Fit to the lifetime formula $\tau=(a/F)\exp(b/F)$ of the data obtained in this experiment is compared with previous experimental results of Jason *et al.* (Ref. [3]), which include the results of Stinson *et al.* (Ref. [1]). The uncertainties (shown in parentheses) for this work are based on a 1σ confidence level in the χ^2 contour. The rest-frame lifetime τ based on the fitting results for a field of 0.5 MV/cm is also shown.

Parameter	This work	Jason *et al.*
a (10^{-6} s V/m)	3.073(10)	2.47(10)
b (10^9 V/m)	4.414(10)	4.49(1)
reduced χ^2	1.18	1.1
τ (10^{-11} s)	4.19	3.92

the other two parametrizations. Table I shows the best-fit results for $P1$ to our data. The strong correlation between the fitting coefficients, noted by Jason *et al.*, is shown in Fig. 2(a). The correlation is due to the presence of the value of the binding energy in both coefficients.

By taking into account the field dependence of the preexponential factor, a better fit to the data was obtained. Table II shows the results of the fits using the parametrization $P2$. The minimum reduced χ^2 for this parametrization was 1.09, an improvement over the previous parametrization. The difference in the best-fit parameters for the two parametrizations reflects the inclusion of the field dependence of the preexponential term. Again there is correlation between the fitting coefficients. The binding energy ε obtained from the fit using the value of the coefficient $a_F=4.448\times10^9$ V/m (neglecting the dependence of the binding energy on the preexponential term) was 0.751 eV, as compared to the lower value of 0.747 eV determined from the parameter $a=4.414\times10^9$ V/cm of $P1$. The lower reduced χ^2 value and the better agreement of the binding energy with the theoretical value make the second parametrization preferable to the first for this range of fields.

The results for the lifetimes based on parametrization $P3$ were similar to those for the parametrizations $P1$ and $P2$. Since the Scherk theory was developed for a weak field, it was instructive to investigate how well the theory agreed with the experimental data as a function of field. Figure 3(a) shows the entire experimental spectrum. Figure 3(b) shows the part of the spectrum derived from H^- stripping plotted with the best fit of the theory for $P3$ at 797 MeV. The differences between the experimental data and the results of the fits divided by the standard deviations of the experimental points (the residuals) are also shown. There is no systematic deviation from the theory for the fields we investigated, as indicated by the randomness of the residuals. The χ^2 contour plot for parametrization $P3$ at 797 corresponding to Fig. 3(b) is shown in Fig. 3(d).

TABLE II. Fit of experimental data obtained in this work using the parametrization $P2$, $\tau=[a_F/(1-\eta F)F]\exp(b_F/F)$. The uncertainties are shown in parentheses.

Parameter	This work	Scherk theory
a_F (10^{-6} s V/m)	2.653(10)	2.66
b_F (10^9 V/m)	4.448(7)	4.474

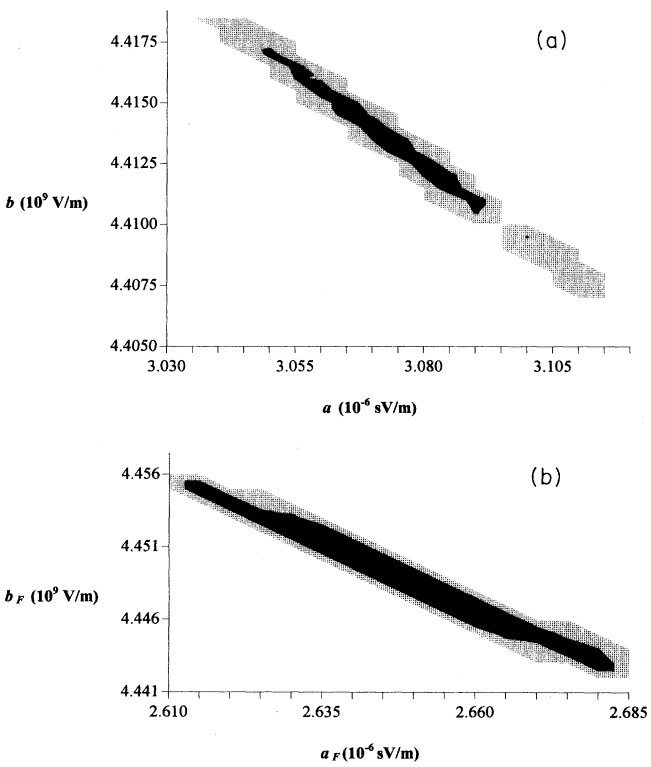

FIG. 2. The χ^2 contour plots for the fits of the two parametrizations of the lifetime formula (a) $\tau=(a/F)\exp(b/F)$ and (b) $\tau=[a_F/(1-\eta F)F]\exp(b_F/F)$ for a beam energy of 797 MeV. The darker interior region is the 1σ confidence interval, and the outer gray region is the 2σ confidence interval. The jagged nature of the confidence intervals reflects the graininess of the calculations.

The minimum reduced χ^2 was 1.11 for $P3$, nearly the same as for $P2$. The χ^2 analysis for this parametrization gave a value for the parameter of ε of 0.752 35(35) [which gives an electron affinity of 0.752 75 eV, 0.3% lower than the experimental value of Lykke *et al.* (Ref. [5])] and a value of $S_0=0.783(5)$ in reasonable agreement with the value 0.794 from the 49-parameter wave-function calculation of Scherk (the 20-parameter wave-function calculation of Scherk gave a value of 0.806). The maximum of the probability density distribution function occurred at a field of 5.0256 MV/cm, which corresponds to a laboratory magnetic-field strength of 1.084 T. The lifetime at the peak was estimated to be 4.047×10^{-11} s.

B. Lifetime of H^- as a function of rest-frame electric field

The lifetime of the H^- ion against field detachment in a static electric field is shown in Fig. 4. The lifetime shown there was calculated using the average of the best fits of parametrization $P3$ for the beam energies 795, 797, and 799 MeV. The uncertainty was calculated by adding in quadrature the uncertainties of the lifetimes for the three beam energies as follows:

$$\delta\tau(F)=\tfrac{1}{3}\sqrt{[\delta\tau_1(F)]^2+[\delta\tau_2(F)]^2+[\delta\tau_3(F)]^2}, \quad (9)$$

where subscripts 1, 2, and 3 refer to beam energies 795, 797, and 799 MeV, respectively. The uncertainty for a given beam

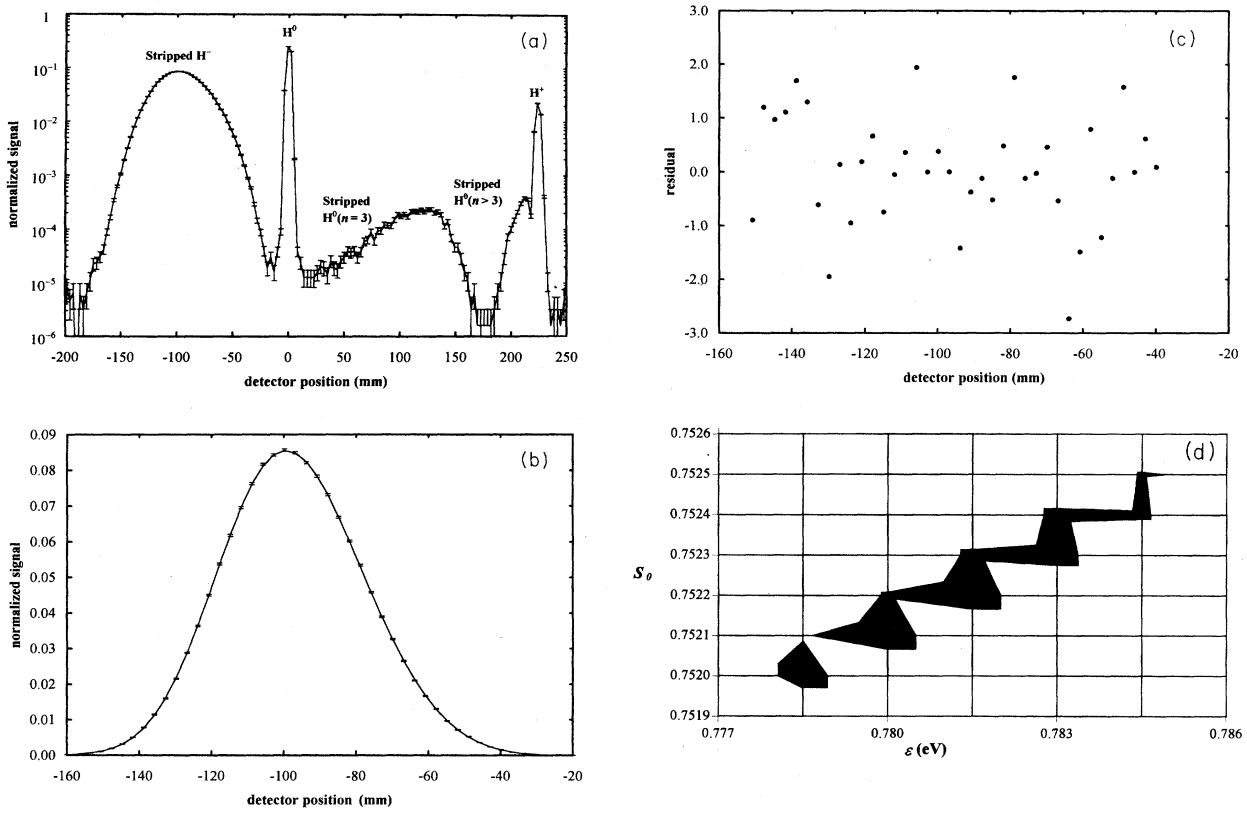

FIG. 3. Results of the fits using the parametrization $P3$ of Eq. (8). (a) The entire normalized spectrum $(H2 \bullet S1 \bullet S2)/(S1 \bullet S2)$ vs x plotted on a log scale. (b) The best fit to the experimental data (linear scale) is shown as a solid line through the experimental data points. The vertical error bars indicate one standard deviation. (c) Solid circles denote the difference between the best fit of the theory and the experimental data divided by the standard deviation for each data point (the residual). (d) The black area represents the 1σ confidence region of the χ^2 contour plot for the best fit corresponding to the plot of (b). The jagged nature of the contour plot reflects the graininess of the calculations.

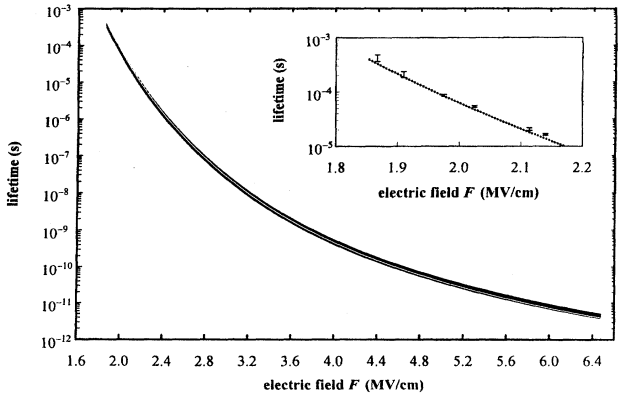

FIG. 4. Plot of the lifetime against electron detachment of $H^-(1s^2\ ^1S)$ vs rest-frame electric field. The best fit of the Scherk theory (Ref. [2]) to data obtained in this work is shown as a solid black line whose thickness is the uncertainty in the lifetime. The results of Jason *et al.* (Ref. [3]) are shown as a white line overlapped by the black line. The low-field data and standard deviations (denoted by I) of Stinson *et al.* (Ref. [1]) are shown in the inset with the results of our study depicted as a smooth line with vertical ticks indicating the uncertainty. The uniform spacing of the standard deviations along the field axis of our results represents the step size used in the calculations.

energy was given by the absolute difference between the lifetime with the coefficients of best fit that gave the highest and lowest values of the lifetime, based on the 1σ confidence region of the χ^2 contour.

Despite the differences in parametrizations, the lifetime as a function of field agrees well with the previous results of Jason *et al.* The lifetime values of Stinson *et al.* are higher on average than those obtained in this work in the low-field region, as shown in Fig. 4.

C. Results of the analysis of the Stinson *et al.* data

The results of the fits to the Stinson *et al.* data for $P1$ and $P2$ are presented in Table III. The minimum reduced χ^2 values of all fits of the Stinson *et al.* data were higher than those obtained for the same fits to the present experimental work and the work of Jason *et al.* The inclusion of the field dependence in $P2$ did not make as significant a difference to the values of the coefficients as it did for the values determined from this work since the field strengths in the Stinson *et al.* work were at the low end of the field range. These results of the parameter fits do not agree with the results of our work, nor do they agree with the Scherk theory. These experimental points were included in the results reported by Jason *et al.*, but were not incorporated in our data.

TABLE III. Fits of the Stinson *et al.* data (Ref. [1]) for the parametrizations $P1$, $\tau=(a/F)\exp(b/F)$ and $P2$, $\tau=[a_F/(1-\eta F)F]\exp(b_F/F)$. The lifetimes were measured in two different ways, called the "strip" and "integral" methods. The value of the minimum χ^2 per degree of freedom (reduced χ^2) is also shown. The uncertainties given in parentheses are the ranges of values for which the χ^2 value increased by 1 from the minimum value. These values of a are higher than, and the values of b lower than, the values for a and b determined in the present experiment and in the experiment of Jason *et al.*, despite the fact that in the latter case, the data of Stinson *et al.* were included.

$\tau=(a/F)\exp(b/F)$			$\tau=[a_F/(1-\eta F)F]\exp(b_F/F)$		
parameter	strip	integral	parameter	strip	integral
a (10^{-6} s V/m)	6.9(2.1)	7.9(2.7)	a_F (10^{-6} s V/m)	6.5(2.0)	7.3(2.4)
b (10^9 V/m)	4.296(64)	4.269(84)	b_F (10^9 V/m)	4.316(66)	4.279(71)
reduced χ^2	4.46	2.30	reduced χ^2	4.45	2.29

The fit of the Stinson *et al.* data to $P3$ produced values of the fit parameters S_0 and ε considerably lower than the theoretical values, and reduced χ^2 values higher than those obtained for the data of this work. The parameter S_0 determined from the fits was nearly three times smaller than the calculated value, and in disagreement with the present results. In a second set of calculations, the parameter S_0 was fixed at 0.794 (the value calculated by Scherk), and the parameter ε was determined for both sets of Stinson *et al.* results. The "strip" method gave the value of $\varepsilon=0.754\,73(71)$ eV with a reduced χ^2 of 5.70, and the "integral" method gave $\varepsilon=0.754\,94(25)$ eV with a reduced χ^2 of 3.74. Adding the contribution of the level shift (estimated by Scherk to be $-0.000\,41$ eV), the electron affinity ε_a of the H^- ion based on the "integral" method value is 0.755 35(41), about 0.15% higher than the measured value of Lykke *et al.* These values for the electron affinity are for the case where all parameters except ε were held fixed. Even with these constraints imposed, the reduced χ^2 values were much higher than those obtained in the Jason *et al.* study and in our work.

D. Experiments for detecting H^- excited states

The experimental technique used in this work may be able to be used to detect putative long-lived (~ 1 ns) excited states of H^- below the H ($n=2$) threshold. Each of these states is very weakly bound and would strip at low fields, appearing as a shoulder on the peak due to undeflected H^0 states. About half of the $2p^2\,{}^3P^e$ state population with a 1.73-ns field-free lifetime produced in a foil one-half meter upstream of the Gypsy magnet would decay before the magnet.

The surviving excited-state ions would bend slightly in the fringe field of the Gypsy magnet before stripping and could possibly be detected downstream. We used the recent calculational results of Ho [11] to investigate whether we could observe any of these excited states with the apparatus described in the present work.

The lifetimes of the various excited states were reported by Ho at discrete field values. We fit the lifetime values of the $M=0$ component of $2p^2\,{}^3P^e$ and the $M=\pm 1$ components of $2s3p\,{}^3P^o(2)$, the two most robust states against field detachment, to the functional form of $P1$ [Eq. (5)]. The lifetimes of the other states reported by Ho were so short that they would strip almost immediately in the Gypsy fringe field and would be indistinguishable from the central H^0 peak. The best fit of the $M=0$ component of the $2p^2\,{}^3P^e$ state was $a=1.073\times10^{-4}$ s V m^{-1} and $b=6.731\times10^{-7}$ V/m, and $a=1.289\times10^{-4}$ s V/m and $b=3.516\times10^{-7}$ V/m for the $M=\pm1$ components of the $2s3p\,{}^3P^o(2)$ state. The fitted lifetimes of these states were used to calculate the probability density distribution functions calculated through the Gypsy magnet for peak fields of 0.6 and 1.3 T. The 0.6-T field setting was used in the related foil experiments (see Ref. [6]). The results are shown in Fig. 5. The peaks of the probability density distributions for these two states through a 1.3-T peak Gypsy field would appear about 3 mm away from the H^0 peak, but almost overlap each other. It is possible that with a fine step size, a narrow detector, and a well-collimated beam, a peak this far from the central H^0 peak could be distinguished. However, particles detected here could also come from a halo beam due to gas stripping, and from H^0 ($n=3$) Stark states stripped in the rest-frame electric field of the Gypsy magnet. Further, since these peaks

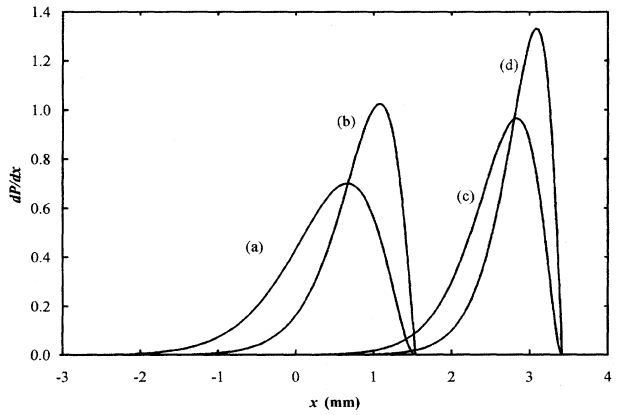

FIG. 5. Predictions for probability density distribution functions using the present experimental apparatus for the $M=0$ component of the $2p^3\,{}^3P^e$ and the $M=\pm1$ components of the $2s3p\,{}^3P^o(2)$ states of H^- for Gypsy magnet peak field settings of 0.6 and 1.3 T. The lifetime values are based on fitting the calculational results of Ho (Ref. [12]) to the function $\tau=(a/F)\exp(b/F)$. Curves (a) through (d) are for the following states and field values: (a) $2p^2\,{}^3P^e$ at 0.6 T, (b) $2s3p\,{}^3P^o(2)$ at 0.6 T, (c) $2p^2\,{}^3P^e$ at 1.3 T, and (d) $2s3p\,{}^3P^o(2)$ at 1.3 T. The x locations of the peaks of the curves are at 0.65, 1.40, 2.83, and 3.02 mm, with FWHM values of 1.4, 1.07, 0.70, and 0.86 mm, respectively.

nearly overlap, deconvolving them from each other would add uncertainty in determining the absolute fractions of these states.

In order to distinguish the dP/dx curve due to excited states of the H^- state from the unstripped H^0 peak, independent measurements of the beam profile and detector response function would have to be made. A narrow scintillator taking data in very fine steps, and a very well collimated H^- beam would be needed for the experiment. Also, since a halo beam of neutral H^0 produced during gas stripping may dominate the signal from the excited-state H^- signal, it is imperative to reduce the background pressure as much as possible.

The $2p^2\ ^3P^e$ state could also be revealed in a photodetachment experiment. Theoretical predictions of the photodetachment cross section for the process

$$H^- 2p^2(^3P^e) + \gamma \rightarrow H(2s,2p) + e^- \tag{10}$$

have been reported recently [12] and compared with earlier work [13]. Ho's semiempirical, adiabatic hyperspherical calculations with photon energies from threshold to 3.40 eV predicted a detachment cross section of 428 Mb at 25.7 meV above threshold. A relativistic H^- beam could interact with a thin foil where the excited H^- states would be produced by collisions with foil atoms. Immediately downstream, the ion beam would be intersected with laser light as has been done in a previous series of experiments [14]. By changing the intersection angle of the ion and light beam, the rest-frame frequency of the light would change and the cross section for the process could be mapped out by measuring the photodetached electrons. For a 10.6-μm (CO_2) laser beam intersecting at 90° to an 800-MeV H^- beam, the center-of-mass photon energy is 0.22 eV, corresponding to a cross section [13] of about 2 Å^2.

The photodetachment technique could prove to be more sensitive than the experiment described above since it does not require separating peaks due to the excited state of H^- from the nearby H^0 peak and the signal from the electric-field stripping of excited H^0 states. The photodetachment experiment's results would not depend on the H^0 signal produced from gas stripping. For these reasons, the photodetachment technique is preferable to the electric-field detachment techniqued in this work.

VI. CONCLUSIONS

The lifetime of the H^- ion in an electric field has been measured over a range of eight orders of magnitude and has been compared with previous results. The lifetime as a function of electric-field strength derived by Scherk agrees reasonably well with our experimental values based on fitting the probability density distribution function for stripped H^-. Three different parametrizations of the lifetime formula of Scherk, $P1$, $P2$, and $P3$ were used. A detailed analysis of the probability density distribution function reveals that the Scherk theory does not show systematic deviation from the experimental values for fields employed here. The lifetime as a function of field agreed within error bars with the previous results of Jason *et al.*, although the fitting coefficients do not agree within error bars. Taking into account the field-dependent prefactor $1-\eta F$ in parametrization $P2$ improved the fit to our data. An estimate of the electron affinity agreed reasonably well with the measured value of Lykke *et al.*, and the value of the parameter S_0 agreed reasonably well with the calculation of Scherk. A finer step size in the magnet map improved the agreement between theory and our experimental results.

Also, the data of Stinson *et al.* were analyzed based on the same three parametrizations of the lifetime formula. The results for the parameters of $P1$ and $P2$ did not agree with the present work, nor with the Scherk theory. When parametrization $P3$ was used, where S_0 and ε were allowed to vary, the results gave a much lower value for the parameter S_0 than was obtained in our work and was estimated by Scherk. When only the parameter ε was allowed to vary, a reasonable estimate of the electron affinity was obtained.

The possibility of observing long-lived H^- excited states was considered. We saw no evidence of excited states of H^- in our data. Although a more sensitive version of the field stripping technique used in this work might reveal such excited states, photodetachment is probably the preferred technique.

ACKNOWLEDGMENTS

We would like to express our appreciation to the Los Alamos technical staff for its invaluable assistance with the setting up and running of the experiment, and to Jim Hontas, John DeMoss, and Karl Allen of the University of New Mexico Physics and Astronomy Shop for their expertise in building the scintillator stage. P.B.K. wishes to thank both J. M. McIver of the University of New Mexico for helpful discussions of data analysis, and A. J. Jason of the Los Alamos National Laboratory for providing detailed explanations of his experimental results. The work was supported by the U.S. Department of Energy, in part by the Division of Chemical Sciences, Office of Basic Energy Sciences, Office of Energy Research.

[1] G. M. Stinson, W. C. Olsen, W. J. McDonald, P. Ford, D. Axen, and E. W. Blackmore, Nucl. Instrum. Methods **74**, 333 (1969); G. M. Stinson, W. C. Olsen, W. J. McDonald, P. Ford, D. Axen, and E. W. Blackmore, TRIUMF Report TRI-69-1 (unpublished).

[2] Leonard R. Scherk, Can. J. Phys. **57**, 558 (1979).

[3] Andrew J. Jason, Daniel W. Hudgings, and Olin B. van Dyck, IEEE Trans. Nucl. Sci. **NS-28**, 2704 (1981).

[4] C. L. Pekeris, Phys. Rev. **112**, 1649 (1958).

[5] K. R. Lykke, K. K. Murray, and W. C. Lineberger, Phys. Rev. A **43**, 6104 (1991).

[6] M. S. Gulley *et al.* (unpublished).

[7] E. Holøien, J. Chem. Phys. **33**, 301 (1960); Phys. Norvegica **1**, 53 (1961–1962).

[8] G. W. F. Drake, Phys. Rev. Lett. **24**, 126 (1970).

[9] T. Tietz, Phys. Rev. **124**, 493 (1961).

[10] W. H. Press, S. A. Teukolsky, W. T. Vetterling, and B. P. Flannery, *Numerical Recipes in C: The Art of Scientific Computing*, 2nd ed. (Cambridge University Press, Cambridge, 1992).
[11] Y. K. Ho, J. Phys. B (to be published).
[12] N.-Y. Du, A. F. Starace, and M.-Q. Bao, Phys. Rev. A **50**, 4365 (1994).
[13] V. L. Jacobs, A. K. Bhatia, and A. Temkin, Astrophys. J. **242**, 1278 (1980).
[14] M. Halka *et al.*, Phys. Rev. A **48**, 419 (1993).